MODELING AND ESTIMATION OF MATERIAL AND BOUNDARY PARAMETERS FOR AN IMPERFECTLY CLAMPED PLATE [1]

H.T. Banks
Center for Research in Scientific Computation
North Carolina State University
Raleigh, NC 27695

Ralph C. Smith
Department of Mathematics
Iowa State University
Ames, IA 50011

Yun Wang
Mathematical Products Division
Armstrong Laboratory
Brooks AFB, TX 78235

1 Introduction

We consider here the problem of modeling inexact boundary conditions when using partial differential equations to describe the dynamics of structures such as beams, plates and shells. When analyzing such structures, it is common to assume ideal edge conditions which leads to the use of fixed-end (zero displacement and slope) or simple (zero displacement and moment) boundary conditions. In applications, however, such conditions are rarely attained due to constraints and limitations in materials, clamping mechanisms, et cetera. This can lead to significant changes in structural dynamics. For example, energy loss through an imperfect clamp can lead to natural frequencies that are 20−30% below those predicted by a model in which fixed boundary conditions are assumed [8]. This discrepancy between the model and actual physical structure can lead to spurious results when performing simulations and degradation and potential destabilization when the model is incorporated in a PDE-based controller.

In collaboration with D.E. Brown, V.L. Metcalf and R.J. Silcox, Acoustics Division, NASA Langley Research Center, we have been investigating modeling, parameter estimation, and control issues in the context of a clamped circular plate with surface-mounted piezoceramic patches. In this lecture, we consider advantages and limitations associated with the use of the model presented in [4] to model edge physics for this plate (the reader is referred to [5, 7, 9] for other approaches for this problem). An outline of the model, discretization techniques and parameter estimation method are given with further details contained in [1]. Parameters in the model are then determined through least squares techniques using accelerometer data from the experimental plate, and the model response is compared with the data. This provides an initial test regarding the suitability of the model for describing the physics of the experimental plate.

2 Modeling Equations

We outline here a weak form of the model for a partially clamped thin circular plate of radius a and thickness h with piezoceramic patches bonded in pairs to its surface. The region occupied by the unstrained neutral surface of the plate is denoted by Γ_0. The piecewise constant density, Young's modulus, Poisson ratio, Kelvin-Voigt and air damping parameters are denoted by ρ, E, ν, c_D and γ, respectively. Displacement in the transverse direction is indicated by w while external surface loads are represented by f. Thus $\Gamma_0 = \{(r, \theta, w) : 0 \leq r \leq a, 0 \leq \theta \leq 2\pi, w = 0\}$.

To provide a framework which facilitates analysis, approximation and implementation, it is advantageous to consider a weak form of the modeling equations. To this end, we take the state $z = (w(a, \cdot), w(\cdot, \cdot))$ in the space $H \equiv L^2(0, 2\pi) \times L^2(\Gamma_0)$ (see [4] for details). A suitable space for test functions is $V = \{\Psi = (\xi(\cdot), \eta(\cdot, \cdot))) \in H : \eta \in H^2(\Gamma_0), \eta(a, \theta) = \xi(\theta)\}$.

[1] The research of H.T.B. and Y.W. (while at NCSU) was supported in part by the Air Force Office of Scientific Research under grant AFOSR-F49620-93-1-0198. This research was also supported by the National Aeronautics and Space Administration under NASA Contract Number NAS1-19480 while all three authors were visiting scientists at the Institute for Computer Applications in Science and Engineering (ICASE), NASA Langley Research Center, Hampton, VA 23681. Additional support for R.C.S. was also provided in part under NASA grant NAG-1-1600. The research of Y.W. at Armstrong Laboratory was also supported in part by the Air Force Office of Scientific Research, Mathematics and Geosciences Directorate.

As detailed in [4], a weak form of the model for an axisymmetric plate is then

$$
\begin{aligned}
&\int_{\Gamma_0} \rho h \frac{\partial^2 w}{\partial t^2}\overline{\eta} d\gamma + \int_{\Gamma_0} \gamma \frac{\partial w}{\partial t}\overline{\eta} d\gamma - \int_{\Gamma_0} M_r \overline{\frac{\partial^2 \eta}{\partial r^2}} d\gamma \\
&- \int_{\Gamma_0} \frac{1}{r^2} M_\theta \left[r\overline{\frac{\partial \eta}{\partial r}} + \overline{\frac{\partial^2 \eta}{\partial \theta^2}} \right] d\gamma \\
&-2\int_{\Gamma_0} \frac{1}{r^2} M_{r\theta} \left[r\overline{\frac{\partial^2 \eta}{\partial r \partial \theta}} - \overline{\frac{\partial \eta}{\partial \theta}} \right] d\gamma \\
&+ \int_0^{2\pi} a \left[k_t w(t,a,\theta) + c_t \frac{\partial w}{\partial t}(t,a,\theta) \right] \overline{\eta}(a,\theta) d\theta \\
&+ \int_0^{2\pi} a\rho h \frac{\partial^2 w}{\partial t^2}(t,a,\theta)\overline{\eta}(a,\theta) d\theta \\
&+ \int_0^{2\pi} a \left[k_p \frac{\partial w}{\partial r}(t,a,\theta) + c_p \frac{\partial^2 w}{\partial r \partial t}(t,a,\theta) \right] \overline{\frac{\partial \eta}{\partial r}}(a,\theta) d\theta \\
&= -\int_{\Gamma_0} \sum_{i=1}^{s} \mathcal{K}_i^B u_i(t) \chi_i(r,\theta) \overline{\nabla^2 \eta} d\gamma + \int_{\Gamma_0} f\overline{\eta} d\gamma
\end{aligned}
\tag{1}
$$

for all $\Psi = (\eta(a,\cdot), \eta(\cdot,\cdot)) \in V$. The overbar here denotes complex conjugation and the differential is $d\gamma = r d\theta dr$. A typical internal plate moment is given by

$$
\begin{aligned}
M_r = \; & -D\left(\frac{\partial^2 w}{\partial r^2} + \frac{\nu}{r}\frac{\partial w}{\partial r} + \frac{\nu}{r^2}\frac{\partial^2 w}{\partial \theta^2} \right) \\
& -c_D\left(\frac{\partial^3 w}{\partial r^2 \partial t} + \frac{\nu}{r}\frac{\partial^2 w}{\partial r \partial t} + \frac{\nu}{r^2}\frac{\partial^3 w}{\partial \theta^2 \partial t} \right)
\end{aligned}
$$

(see [3, 6] for details regarding the derivation of the moment expressions M_r, M_θ and $M_{r\theta}$). As discussed in [3], the density ρ and parameters $D = \frac{Eh^3}{12(1-\nu^2)}, \nu$ and c_D in the moment expressions are discontinuous due to the geometrical and material changes resulting from the bonding of the patches to the plate.

The active contributions due to s piezoceramic patches and a driving force f are modeled by the right hand side components. Here $\chi_i(r,\theta)$ denotes the characteristic function which has a value of 1 in the region covered by the i^{th} patch and is 0 elsewhere. Moreover, $u_i(t)$ is the voltage into the i^{th} patch and $\mathcal{K}_i^B$ is a parameter which depends on the geometry, piezoceramic material properties and piezoelectric strain constants (see [3] for details).

As discussed in [4], the boundary conditions in the sixth and eighth components of (1) admit slight displacements and rotations at the boundary $r = a$. The parameters k_t and c_t denote stiffness and damping contributions when boundary displacement occurs with similar interpretations for k_p and c_p when accounting for boundary rotation. In applications, the boundary parameters k_t, c_t, k_p, c_p, the piezoceramic material parameters $\mathcal{K}_i^B, i = 1, \cdots, s$, and the plate parameters ρ, D, ν, c_D and γ should be considered as unknown and must be estimated using fit-to-data techniques.

3 State Approximation

The state and test functions in (1) are infinite dimensional and must be approximated before parameter estimation and control methods can be implemented. As discussed in [2, 10], an appropriate choice for basis and Fourier-Galerkin expansion of the plate displacement is $B_k^{\mathcal{N}}(r,\theta) = r^{|\hat{m}|} B_n^m(r) e^{im\theta}$ and

$$
\begin{aligned}
w^{\mathcal{N}}(t,r,\theta) &= \sum_{m=-M}^{M} \sum_{n=1}^{N^m} w_{mn}^{\mathcal{N}}(t) r^{|\hat{m}|} B_n^m(r) e^{im\theta} \\
&= \sum_{k=1}^{\mathcal{N}} w_k^{\mathcal{N}}(t) B_k^{\mathcal{N}}(r,\theta) \; .
\end{aligned}
\tag{2}
$$

Here $B_n^m(r)$ denotes a cubic spline that is modified so as to satisfy the condition $\frac{dB_n^m(0)}{dr} = 0$ when $m = 0$. This guarantees differentiability at the origin and implies that $N^m = N + 2$ when $m = 0$ and $N^m = N + 3$ when $m \neq 0$ where N denotes the number of modified cubic splines. Thus a total of $\mathcal{N} = (2M+1)(N+3) - 1$ basis functions are used when approximating the plate displacement. As discussed in the [2, 10], the inclusion of the weighting term $r^{|\hat{m}|}$ with $\hat{m} = 0$ if $m = 0$, $\hat{m} = 1$ if $m \neq 0$ is motivated by the asymptotic behavior of the Bessel functions (which make up the analytic plate solution) as $r \to 0$. It also serves to ensure the uniqueness of the solution at the origin. The Fourier coefficient in the weight is truncated to control the conditioning of the mass and stiffness matrices (see the examples in [2]).

To obtain a matrix system, the $\mathcal{N}$ dimensional approximating subspace is taken to be $H^{\mathcal{N}} = span\{B_k^{\mathcal{N}}\}$ and the product space for the first-order system is $H^{\mathcal{N}} \times H^{\mathcal{N}}$. The restriction of the infinite-dimensional system (1) to the space $H^{\mathcal{N}} \times H^{\mathcal{N}}$ then yields a matrix system of the form

$$
\begin{aligned}
\dot{y}^{\mathcal{N}}(t) &= A^{\mathcal{N}} y^{\mathcal{N}}(t) + B^{\mathcal{N}} u(t) + F^{\mathcal{N}}(t) \\
y^{\mathcal{N}}(0) &= y_0^{\mathcal{N}}
\end{aligned}
\tag{3}
$$

where $y^{\mathcal{N}}(t) = [w_1(t), \cdots, w_{\mathcal{N}}(t), \dot{w}_1(t), \cdots, \dot{w}_{\mathcal{N}}(t)]$ denotes the $2\mathcal{N} \times 1$ vector containing the generalized Fourier coefficients for the approximate displacement and velocity. Details concerning the construction of the component vectors and matrices in (3) can be found in [2, 10].

4 Parameter Estimation

In order to attain an accurate fit of the model (1) to the experimental apparatus under consideration, the parameters $\rho, D, \nu, c_D, \gamma, k_t, c_t, k_p, c_p, \mathcal{K}_1^B, \cdots, \mathcal{K}_s^B$ must be estimated using experimental data in order to obtain an accurate model fit to an experimental apparatus. One means

of doing so is by minimizing the least squares difference between measurements of the experimental data and the model response. We first summarize assumptions regarding the nature of the parameters being estimated.

Due to the piecewise constant nature of the structure when s patches or patch pairs are bonded to the plate, it is assumed that the parameters ρ, D, ν and c_D can be expressed as

$$\rho(r,\theta) = \sum_{i=1}^{s+1} c_{\rho i}\chi_i(r,\theta) \quad , \quad D(r,\theta) = \sum_{i=1}^{s+1} c_{Di}\chi_i(r,\theta)$$

$$\nu(r,\theta) = \sum_{i=1}^{s+1} c_{\nu i}\chi_i(r,\theta) \quad , \quad c_D(r,\theta) = \sum_{i=1}^{s+1} c_{c_D i}\chi_i(r,\theta) \, .$$

Again, $\chi_i(r,\theta)$, $i = 1, \cdots, s$ is the characteristic function over the i^{th} patch or patch pair and χ_{s+1} is the characteristic function over the portion of the plate not covered with patches. The damping due to air is assumed to be uniform over the entire surface; hence γ is taken to be constant. Moreover, the boundary parameters k_t, c_t, k_p, c_p and patch parameters $\mathcal{K}_1^B, \cdots, \mathcal{K}_s^B$ are assumed to be constant.

For $q = (\rho, D, \nu, c_D, \gamma, k_t, c_t, k_p, c_p, \mathcal{K}_1^B, \cdots, \mathcal{K}_s^B)$ in an admissible parameter space Q which incorporates these constraints (see [4]), the finite dimensional parameter estimation problem is to find $\bar{q} \in Q$ which minimizes

$$J^N(q) = \sum_i \left| \frac{\partial^2 w^{\mathcal{N}}}{\partial t^2}(t_i, \hat{r}, \hat{\theta}; q) - z_i \right|^2 \qquad (4)$$

subject to $w^{\mathcal{N}}$ satisfying the approximate plate equations (hence the coefficients $\{w_k^{\mathcal{N}}\}$ of $w^{\mathcal{N}}$ must satisfy (3)). Data is measured and approximate solutions are calculated at the points $(\hat{r}, \hat{\theta})$ on the plate. The choice of computed acceleration values of the model response is due to the use of accelerometers for data collection on the plate.

In the results of the next example, the minimization of the functional (4) was accomplished via a Levenberg-Marquardt routine with a stiff ODE solver being used to integrate the system (3) in order to obtain the model response at the sample points. This minimization can also be performed with various constrained optimization routines in which case, parameter constraints such as positivity can be enforced.

5 Experimental Example

For the experiment reported here, a thin circular plate (having radius 9″ and thickness .05″) mounted in a heavy frame by a metal collar was considered (see [1] for additional details regarding the experiments). The bolts in the collar were loosened slightly to permit slight energy loss at the plate edge. Bonded to the plate were a pair of centered piezoceramic patches of radius .75″ and thickness .007″.

The plate was excited by a centered strike with an impact hammer and the resulting axisymmetric response was measured by a centered accelerometer on the opposite side of the plate. The data was collected at a rate of 12 KHz so as to resolve all excited frequencies.

The parameters $\rho, D, \nu, c_D, \gamma, k_t, c_t, k_p, c_p$ were estimated through the minimization of the functional (4) and the model response with the estimated parameters is compared with the experimental data in Figures 1 and 2. As noted in Figure 2, the first two frequencies are quite accurately matched whereas the third and fourth modes are overdamped in the model response. The phenomenon of overdamping high frequency modes is characteristic of the Kelvin-Voigt damping model, and this leads to some of the variation seen in the time histories in Figure 1 when comparing the experimental data and model response. The slight variation in the time histories is also due to the fact that the model frequencies for the third and fourth modes are slightly less than the corresponding experimental results. Further results illustrating the use of the boundary moment model are given in [1].

As demonstrated by the results in Figures 1 and 2 as well as a repertoire of examples in [1], the boundary moment model does appear to describe some of the mechanisms leading to the lowering of frequencies when the plate is imperfectly clamped. Depending upon the means of excitation and degree of loosening at the plate edge, other mechanisms such as in-plane movement and friction may contribute to the loss of energy at the plate edge. Results regarding the modeling of these phenomena from a PDE perspective will be reported on in a future work.

References

[1] H.T. Banks, R.C. Smith, Y. Wang, D.E. Brown, V.E. Metcalf and R.J. Silcox, "The Estimation of Material and Boundary Parameters in a PDE-Based Circular Plate Model," preprint.

[2] H.T. Banks and R.C. Smith, "The Modeling and Approximation of a Structural Acoustics Problem in a Hard-Walled Cylindrical Domain," Center for Research in Scientific Computation Technical Report CRSC-TR94-22, book chapter "Numerical Techniques for Simulation, Parameter Estimation and Noise Control in Struc-

tural Acoustic Systems," in *Dynamics and Control of Distributed Systems*, Editors: H.S. Tzou and L.A. Bergman, Cambridge University Press, to appear.

[3] H.T. Banks, R.C. Smith and Y. Wang, "Modeling Aspects for Piezoceramic Patch Activation of Shells, Plates and Beams," to appear in *Quarterly of Applied Mathematics.*

[4] H.T. Banks, R.C. Smith and Y. Wang, "Modeling and Parameter Estimation for an Imperfectly Clamped Plate," to appear in *Computation and Control IV,* Proc. Fourth Bozeman Conf., Bozeman, MT, 1994, Progress in Systems and Control Theory, Birkhäuser Boston, Inc., 1995.

[5] C.M. LaPeter, "Application of Distributed Measurements for Finite Elements Model Verification," Master's Thesis, Virginia Polytechnic Institute and State University, May 1992.

[6] E.H. Mansfield, *The Bending and Stretching of Plates*, Volume 6 in the International Series of Monographs on Aeronautics and Astronautics, The MacMillan Company, New York, 1964.

[7] K.D. Murphy, L.N. Virgin and S.A. Rizzi, "Free Vibration of Thermally Loaded Panels Including Initial Imperfections and Post-Buckling Effects," NASA Technical Memorandum 109097, April 1994.

[8] J. Robinson, Acoustics Division, NASA Langley Research Center, personal communications.

[9] J.H. Robinson, S.A. Rizzi, S.A. Clevenson and E.F. Daniels, "Large Deflection Random Response of Flat and Blade Stiffened Carbon Panels," Proc. of the 33^{rd} AIAA/ASME/ASCE/AHS/ASC Structures, Structural Dynamics and Materials Conference, Dallas, TX, 1992.

[10] R.C. Smith, "A Galerkin Method for Linear PDE Systems in Circular Geometries with Structural Acoustic Applications," ICASE Report No. 94-40, submitted to *SIAM Journal on Scientific Computing.*

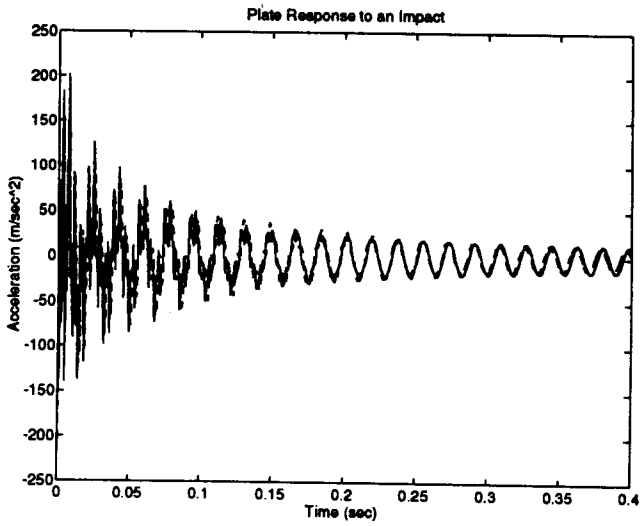

Figure 1. Time history of experimental data and model response; —— (Experimental Data), – – – (Model Response).

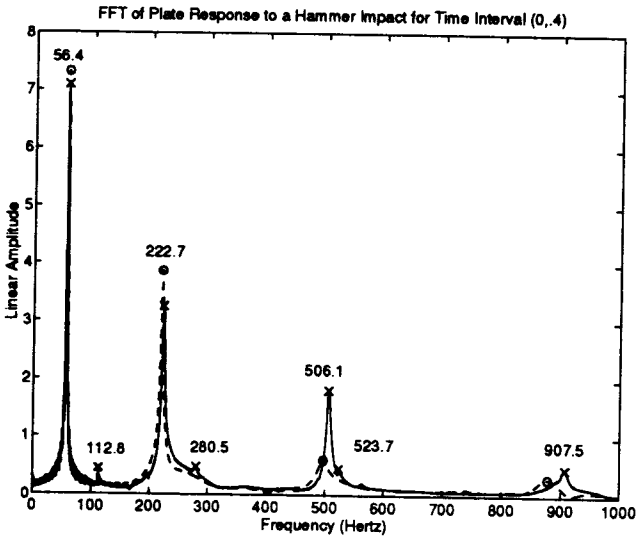

Figure 2. Frequency content of experimental data and model response; x —— (Experimental Data), o – – – (Model Response).